MITSUBISHI ELECTRIC RESEARCH LABORATORIES
https://www.merl.com

Speed Estimation for Contactless Electromagnetic Encoders

Wang, Pu; Orlik, Philip V.; Wang, Bingnan; Sadamoto, Kota; Tsujita, Wataru; Sawa, Yoshitsugu

TR2017-157 October 29, 2017

Abstract

This paper considers speed estimation for contactless electromagnetic (EM) encoder system with a moving readhead and spatially periodic placed reflectors. We first introduce a new signal model to capture reflected signals from these spatially periodic placed reflectors. Then an instantaneous phase-based speed estimator is proposed by using the phase unwrapping technique followed by a nonlinear least square method for motion-related parameters. The proposed speed estimator is verified by 1) Monte-Carlo simulations to confirm its statistical efficiency as the numerical mean squared errors approach to corresponding Cramer-Rao bounds and 2) a semi-analytical dataset by accounting for real system specificaltions such as the antenna beampattern, 3-dB beamwidth, and noise.

IEEE Industrial Electronics Society (IECON) 2017

Mitsubishi Electric Research Laboratories, Inc.
201 Broadway, Cambridge, Massachusetts 02139

Speed Estimation for Contactless Electromagnetic Encoders

Pu Wang, Philip V. Orlik, Bingnan Wang
Mitsubishi Electric Research Laboratories
201 Broadway, Cambridge, MA 02139, USA
Email: pwang@merl.com
Email: porlik@merl.com
Email: bwang@merl.com

Kota Sadamoto, Wataru Tsujita, and Yoshitsugu Sawa
Advanced Technology R&D Center, Mitsubishi Electric Corp.
Amagasaki City, 661-8661, Japan
Email: Sadamoto.Kota@ea.MitsubishiElectric.co.jp
Email: Tsujita.Wataru@eb.MitsubishiElectric.co.jp
Email: Sawa.Yoshitsugu@ct.MitsubishiElectric.co.jp

***Abstract*—This paper considers speed estimation for contactless electromagnetic (EM) encoder system with a moving read-head and spatially periodic placed reflectors. We first introduce a new signal model to capture reflected signals from these spatially periodic placed reflectors. Then an instantaneous phase-based speed estimator is proposed by using the phase unwrapping technique followed by a nonlinear least square method for motion-related parameters. The proposed speed estimator is verified by 1) Monte-Carlo simulations to confirm its statistical efficiency as the numerical mean squared errors approach to corresponding Cramér-Rao bounds and 2) a semi-analytical dataset by accounting for real system specificaltions such as the antenna beampattern, 3-dB beamwidth, and noise.**

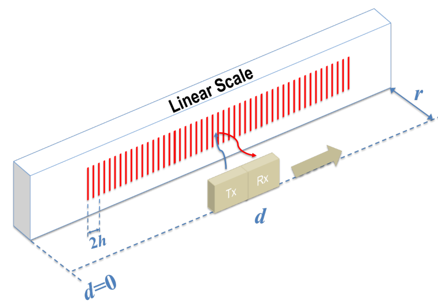

Fig. 1. The geometric configuration of linear electromagnetic encoder systems. The source transceivers are mounted on a moving read-head with a distance to the scale platform. On the scale platform, uniformly spaced bars are installed.

I. Introduction

Encoders, e.g., linear encoders, for precise position and/or speed measurements are required in many applications. The estimated positions can be used as position values for measuring purposes, and fed back to a position control loop. Such encoders are accordingly used in devices such as coordinate measuring machines, geodetic devices, robot arms, radar, sonar, communications, acoustics, optics or hydraulic actuators. Beside the position measurement, accurate speed measurement is also highly desired for the contactless encoder system. Optical, electric conducting (sliding contact) and magnetic encoders are commonly used for high accuracy motion and position measurements in motion control applications such as auto-tuning drives, smart conveyors, and kit motors [1]–[5]. Here, we consider contactless electromagnetic (EM) encoders, which provide robust sensing capability of position and motion in hash operating environments, e.g., moisture, heat, vibration and smoke.

As shown in Fig. 1, the contactless encoder system normally consists of a stationary scale and a moving read-head, or vice versa. The source EM transceivers are mounted on the moving readhead with a distance of r to the scale platform. Uniformly spaced reflectors, e.g., rectangular bars, are installed on the scale platform to constitute a spatial period with an inter-reflector spacing of h. The position encoding is achieved by observing the same reflected EM signals at two spatial positions with a distance of h. A refiner position encoding is also enabled by detecting a fractional phase change between two spatial positions (with a distance less than h) with respect to a full radian period of 2π for a distance of h.

In this paper, we are interested in estimating the speed of the moving read-head by using the contactless encoder system with uniformly spaced reflectors. In principle, the speed can directly be estimated from the relative phase change between two consecutive samples. However, due to the periodic pattern of the reflectors in the scale, a sinusoidal frequency modulated (FM) component is also present in the phase of the reflected signal. Moreover, the sinusoidal FM frequency is speed-dependent. That is, if the read-head moves faster, the sinusoidal FM frequency becomes larger. As a result, the reflected signal is a combination of a polynomial phase signal (PPS) component to capture the motion of the moving read-head and a sinusoidal FM component due to the use of uniformly spaced reflectors.

By taking into account both signal components, we propose a speed estimator by first extracting the phase information of the reflected signal, and then using a nonlinear least square approach to estimate the motion-related phase parameters. Referred to the phase unwrapping least square (PULS) method, the proposed estimator is much faster than the optimal maximum likelihood estimation (MLE) which requires a multi-dimensional search over the nonlinear parameter space. It is further verified with extensive Monte-Carlo simulations and a semi-analytical dataset with real system specifications.

The remainder of this paper is organized as follows. In Section II, we begin with a simple scenario when the read-head moves with a constantly accelerated velocity, and then generalize the signal model for any arbitrary dynamic motion. Section III quickly reviews the optimal MLE for the given signal model and introduces the proposed PULS speed estimator, which is numerically verified in Section IV. A brief summary is given in Section V.

II. Signal Model for Contactless EM Encoders

Given the configuration of Fig. 1, the equivalent baseband signal reflected from the spatially periodic reflectors on the linear scale can be written as

$$x(d) = Ae^{j2\pi\left[\frac{d}{h}+\sum_{m=1}^{M} b_m \sin\left(\frac{2\pi m d}{h}+\phi_m\right)+\psi_0\right]}, \quad (1)$$

where A is the unknown amplitude, d is the axial position index of the moving read-head, $b_m > 0$ and ϕ_m are the modulation index and, respectively, the initial phase of the m-th sinusoidal FM component, M is the number of sinusoidal FM components in the phase, and ψ_0 is the initial phase.

On the right side of (1), the first phase term is due to the fractional phase change proportional to the inter-reflector spacing of h. Therefore, the moving distance and speed of the moving readhead can be inferred from the change in the first phase term. Meanwhile, the second phase term is, induced by the spatially periodic reflectors, the motion-related sinusoidal FM component. From (1), we have $x(d) = x(d+lh)$, where l is an integer. That is the moving read-head receives exactly the same waveforms (in the noiseless case) at two axial positions which are at a distance of (an integer multiple of) h apart from each other.

A. The Constant-Acceleration Case

With a sampling interval of ΔT and assuming that the readhead moves at an initial velocity of v_0 and a constant acceleration of a, we can map the position index to the discrete-time index via $d = v_0 t + at^2/2|_{t=n\Delta T} = v_0 n\Delta T + a(n\Delta T)^2/2, n = n_0, \cdots, n_0+N-1$ with n_0 and N denoting the initial sampling index and the number of total samples, respectively. As a result, the discrete-time version of the reflected signal of (1) is given as

$$\begin{aligned} x(n) =& Ae^{j2\pi\left[\frac{(v_0\Delta T)n+(0.5a(\Delta T)^2)n^2}{h}+\psi_0\right]} \\ &\times e^{j\sum_{m=1}^{M} 2\pi\left[b_m \sin\left(2\pi m \frac{v_0\Delta T n+0.5a(\Delta T)^2 n^2}{h}+\phi_m\right)\right]}, \quad (2) \end{aligned}$$

which consists a second-order motion-induced PPS (i.e., the first exponential term on n) and a sinusoidal FM signal, i.e., the second exponential term. In (2), the sinusoidal FM frequency is now a function of the motion-related phase parameter (e.g., v_0 and a) of the moving read-head.

B. The Generalized Signal Model

To derive the signal model in (2), we assume that the read-head moves at a constant acceleration, i.e., $d = v_0 t + at^2/2|_{t=n\Delta T} = v_0 n\Delta T + a(n\Delta T)^2/2$. For more dynamic motions of the read-head, higher-order phase terms appear in the reflected signal. For instance, if the acceleration is time-varying, a third-order phase term (on t^3) may be required to model the reflected signal, i.e., $d = v_0 t + at^2/2 + gt^3/6$ where g denotes the acceleration rate. To describe any arbitrary dynamic motion, we introduce below a generalized *coupled* mixture of the PPS and sinusoidal FM signals for the contactless EM encoder system

$$x(n) = Ae^{j2\pi\left[\sum_{p=0}^{P}\frac{a_p n^p}{p!}+\sum_{m=1}^{M} b_m \sin(2\pi m f_0(\mathbf{a}_P)n+\phi_m)\right]}, \quad (3)$$

where the fundamental sinusoidal FM frequency f_0 is now coupled with the PPS phase parameters, $\mathbf{a}_P \triangleq [a_1, \cdots, a_P]^T$ with a_p contributing to the dynamic motion of the read-head, e.g., a_1 is proportional to the initial velocity, a_2 is related to the acceleration, and a_3 reflects the acceleration rate. For our application, $f_0(\mathbf{a}_P) = \sum_{p=1}^{P} a_p n^{p-1}/p!$ is a linear function with respect to the PPS phase parameters $\mathbf{a}_P$.

To see how the linear encoder example fits into the coupled mixture of (3), we can establish the following variable changes between (2) and (3)

$$\begin{aligned} &b_m = b_m, \quad a_0 = \psi_0, \quad a_1 = \frac{v_0\Delta T}{h}, \quad a_2 = \frac{a(\Delta T)^2}{h}, \quad (4) \\ &f_0(\mathbf{a}_P) = \frac{v_0\Delta T}{h} + \frac{a(\Delta T)^2}{h} n/2 = a_1 + a_2 n/2, \end{aligned}$$

with a PPS order of $P = 2$ in (3).

C. Relevance to Existing PPS Models

It is worth noting that the above *coupled* mixture model is related to two existing PPS models. One is the *pure* PPS model used often in radar, sonar, communications, acoustics and optics [6]–[9]

$$x(n) = Ae^{j2\pi\sum_{p=0}^{P}\frac{a_p}{p!}n^p} \quad (5)$$

which is a special case of (3) by imposing the FM indices into zeros, i.e., $b_m = 0, m = 1, \cdots, M$. The other is an *independent* mixture of PPS and sinusoidal FM signal, a well-studied signal model found in applications in pulse Doppler radar systems [10]–[13]

$$x(n) = Ae^{j2\pi\left[\sum_{p=0}^{P}\frac{a_p n^p}{p!}+\sum_{m=1}^{M} b_m \sin(2\pi m f_0 n+\phi_m)\right]}, \quad (6)$$

where the FM frequency f_0 is *independent* of the PPS parameters $\{a_p\}_{p=1}^{P}$.

With the generalized signal model given in (3), the problem of interest is to estimate the motion-related parameters $\{a_p\}_{p=1}^{P}$ from a finite number of noisy samples

$$y(n) = x(n) + v(n), n = n_0, n_0+1, \cdots, n_0+N-1, \quad (7)$$

where $x(n)$ is given by (3) and $v(n)$ is assumed to be Gaussian distributed with zero mean and variance σ^2. With the estimated phase parameters $\{a_p\}_{p=1}^{P}$, one can recover the motion-related parameters, e.g., v_0 and a, via (4). In certain applications, other parameters, e.g., A, $\{b_m\}_{m=1}^{M}$ and ϕ_m, may be of interest.

III. Contactless Speed Estimation

We start with a brief review of the maximum likelihood (ML) estimation which is optimal to the signal model in (3), and then introduce the proposed PULS estimator which is computationally more efficient than the ML estimator.

A. Maximum Likelihood Estimator

The ML estimator minimizes the following negative log-likelihood function [14]

$$\Lambda = \frac{\sum_n \left| y(n) - Ae^{j2\pi\left[\sum_{p=0}^{P}\frac{a_p n^p}{p!} + \sum_m b_m \sin(2\pi m f_0(\mathbf{a})n + \phi_m)\right]}\right|^2}{\sigma^2} \tag{8}$$

with respect to A, $\{a_p\}_{p=0}^{P}$, and $\{b_m, \phi_m\}_{m=1}^{M}$. It results in a multi-dimensional search over $(2M + P)$ nonlinear phase parameters of $\{a_p\}_{p=1}^{P}$ and $\{b_m, \phi_m\}_{m=1}^{M}$ [1]. To find the global minimal, the ML estimation in (8) involves a multi-dimensional search and, hence, is computationally prohibited from practical applications. It may converge to a local minimal if the initial guess is far away from the global minimal.

B. Proposed PULS Speed Estimator

The PULS method, on the other hand, is a computationally lighter approach which first extracts the instantaneous phase information from the reflected signal, and then estimates the motion-related parameters from the extracted phase. The flowchart for the proposed PULS estimator is summarized in Fig. 2.

1) Step I: Phase Unwrapping: The first step is to extract the phase of the received signal of (7) and unwrap the extracted phase using a standard phase unwrapping technique,

$$\begin{aligned}\hat{\phi}(n) &= \frac{\angle y(n)}{2\pi}, \quad n = n_0, \cdots, n_0 + N - 1, \\ &= \sum_{p=0}^{P} a_p n^p + \sum_{m=1}^{M} b_m \sin(2\pi m f_0(\mathbf{a})n + \phi_m) + w(n)\end{aligned} \tag{9}$$

where $w(n)$ is the equivalent noise contribution to the unwrapped phase. The phase unwrapping essentially transforms the original signal samples of $y(n)$ into the phase measurements of $\hat{\phi}(n)$ which provide more direct inference on the phase parameters of interest, e.g., a_p and b_m.

[1] A and a_0 are referred to as linear parameters.

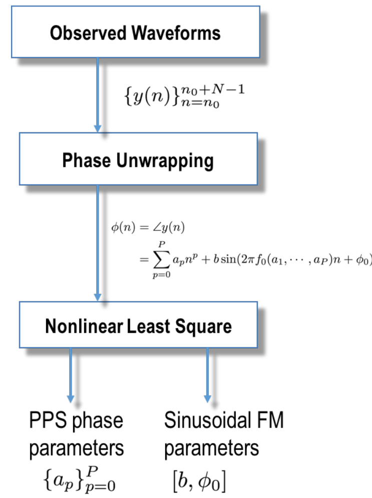

Fig. 2. The flowchart of the phase-based PULS speed estimator.

2) Step II: Nonlinear Least Square: From (9), it is seen that the motion-related parameters, i.e., $\mathbf{a}_P = [a_1, a_2, \cdots, a_P]^T$, are present in the unwrapped phase. More precisely, they appear in both the first term as linear variables and the second term as nonlinear variables via the sinusoidal frequency $f_0(\mathbf{a}_P)$.

To group linear and nonlinear variables in (9), we further expand (9) as follows

$$\begin{aligned}\hat{\phi}(n) =& a_0 + \sum_{p=1}^{P} a_p n^p + \sum_{m=1}^{M} b_m \cos(\phi_m)\sin(2\pi m f_0 n) \\ &+ \sum_{m=1}^{M} b_m \sin(\phi_m)\cos(2\pi m f_0 n) + w(n),\end{aligned} \tag{10}$$

which can be further expressed in a compact vector form below. Specifically, we group $K \leq N$ extracted phase values in (9) into a column vector $\hat{\mathbf{\Phi}} = \left[\hat{\phi}(n_0), \cdots, \hat{\phi}(n_0 + K - 1)\right]^T$. By defining the following vectors and matrices

$$\begin{aligned}\mathbf{A}_P &= [\mathbf{n}_1, \mathbf{n}_2, \cdots, \mathbf{n}_P], \quad \mathbf{S}_M = [\mathbf{s}_1, \mathbf{s}_2, \cdots, \mathbf{s}_M], \\ \mathbf{C}_M &= [\mathbf{c}_1, \mathbf{c}_2, \cdots, \mathbf{c}_M], \\ \mathbf{t} &= [a_0, \quad b_1\cos(\phi_1), \cdots, b_M\cos(\phi_M), \\ &\quad\quad b_1\sin(\phi_1), \cdots, b_M\sin(\phi_M)]^T,\end{aligned} \tag{11}$$

where $\mathbf{n}_p = [n_0^p, \cdots, (n_0 + K - 1)^p]^T$, and

$$\mathbf{s}_m = [\sin(2\pi m f_0(\mathbf{a}_P)n_0), ..., \sin(2\pi m f_0(\mathbf{a}_P)(n_0 + K - 1))]^T,$$
$$\mathbf{c}_m = [\cos(2\pi m f_0(\mathbf{a}_P)n_0), ..., \cos(2\pi m f_0(\mathbf{a}_P)(n_0 + K - 1))]^T,$$

(9) can be rewritten as

$$\hat{\mathbf{\Phi}} = \mathbf{A}_P\mathbf{a}_P + [\mathbf{1}, \mathbf{S}_M, \mathbf{C}_M]\mathbf{t} \triangleq \mathbf{A}_P\mathbf{a}_P + \mathbf{H}_{\mathbf{a}_P}\mathbf{t} \tag{12}$$

where $\mathbf{H}_{\mathbf{a}_P} = [\mathbf{1}, \mathbf{S}_M, \mathbf{C}_M]$ with $\mathbf{1}$ denoting an all-one vector. Note that $\mathbf{a}_P$ appears in (12) not only in a linear form (the first term) but also in a nonlinear form via $\mathbf{S}_M$ and $\mathbf{C}_M$.

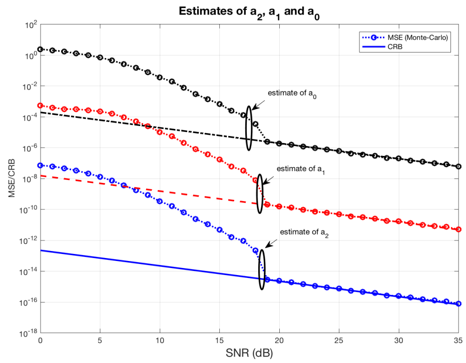

Fig. 3. The measured MSE of the proposed PULS estimator and corresponding CRBs for estimating a_2, a_1 and a_0 from a finite number of samples $N = 512$.

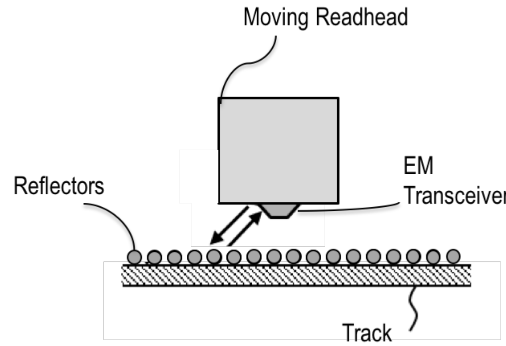

Fig. 4. A semi-analytical simulator with real system specifications such as the radiation angle, 3-dB beam width, and transmitting beam pattern.

With (12), the nonlinear least square approach is to minimize the following cost function with respect to the unknown parameters $\mathbf{a}_P$ and $\mathbf{t}$

$$[\hat{\mathbf{a}}_P, \hat{\mathbf{t}}] = \arg\min_{\mathbf{a}_P, \mathbf{t}} \|\hat{\mathbf{\Phi}} - \mathbf{A}_P \mathbf{a}_P - \mathbf{H}_{\mathbf{a}_P} \mathbf{t}\|^2. \tag{13}$$

If $\mathbf{a}_P$ is known, so is $\mathbf{H}_{\mathbf{a}_P}$. Then the remaining unknown parameter $\mathbf{t}$ can be estimated in closed form

$$\hat{\mathbf{t}} = \left(\mathbf{H}_{\mathbf{a}_P}^T \mathbf{H}_{\mathbf{a}_P}\right)^{-1} \mathbf{H}_{\mathbf{a}_P}^T \left(\hat{\mathbf{\Phi}} - \mathbf{A}_P \mathbf{a}_P\right). \tag{14}$$

Replacing the above estimate of $\mathbf{t}$ back to the cost function of (13), the parameter $\mathbf{a}_P$ can be estimated by solving the following cost function

$$\begin{aligned} \hat{\mathbf{a}}_P &= \min_{\mathbf{a}_P} \|\hat{\mathbf{\Phi}} - \mathbf{A}_P \mathbf{a}_P - \mathbf{H}_{\mathbf{a}_P} \hat{\mathbf{t}}\|^2 \\ &= \min_{\mathbf{a}_P} \left(\hat{\mathbf{\Phi}} - \mathbf{A}_P \mathbf{a}_P\right)^T \mathbf{P}_{\mathbf{H}_{\mathbf{a}_P}}^{\perp} \left(\hat{\mathbf{\Phi}} - \mathbf{A}_P \mathbf{a}_P\right) \end{aligned} \tag{15}$$

where $\mathbf{P}_{\mathbf{H}_{\mathbf{a}_P}}^{\perp} = \mathbf{I} - \mathbf{H}_{\mathbf{a}_P} \left(\mathbf{H}_{\mathbf{a}_P}^T \mathbf{H}_{\mathbf{a}_P}\right)^{-1} \mathbf{H}_{\mathbf{a}_P}^T$ is a projection matrix which projects into the orthogonal complement of the range space of $\mathbf{H}_{\mathbf{a}_P}$. With $\hat{\mathbf{a}}_P$ and $\hat{\mathbf{t}}$, the phase parameters are all estimated. Finally, the estimated phase parameters $\hat{\mathbf{a}}_P$ can be mapped back to the motion parameters, e.g., the initial velocity and acceleration, by using (4).

C. Statistical Bound for Phase Parameter Estimation

In [15], statistical performance bounds in terms of the Cramér-Rao bound (CRB) on the parameter estimation have been derived. It reveals that, on one hand, the derived CRB is dependent on both PPS-related and sinusoidal FM-related parameters, different from the pure PPS case where the CRB is independent of the PPS-related parameters. On the other hand, the derived CRBs for the PPS-related parameters are lower than their counterparts of the independent mixture model, as the sinusoidal FM frequency provides additional information on the PPS-related parameters. In other words, joint estimation of the motion-related parameters can lead to more accurate result from the coupled mixture model than the traditional independent mixture model.

IV. Performance Evaluation

In this section, simulation results are provided to demonstrate the performance of the proposed PULS speed estimator. In the noisy scenario, the signal-to-noise ratio (SNR) is defined as $\text{SNR} = A^2/\sigma^2$.

A. Monte-Carlo Validation

We first synthesize a mixture signal of a single sinusoidal FM component ($M = 1$) and a PPS with order $P = 2$, according to (3), i.e., a constant acceleration model. Other parameters are $A = 1$, $a_0 = 0$, $a_1 = 0.15$, $a_2 = 1.3889 \cdot 10^{-4}$, $b_1 = 0.05$, $\phi_1 = 0$, $c_0 = 0.1$ and $N = 512$. For the coupled mixture signal of (3), the sinusoidal FM frequency is determined by $f_0(a_1, a_2) = a_1 + a_2 n/2$. The ML estimator is known to achieve the CRB asymptotically, but it involves a multi-dimensional search (e.g., a four-dimension search on (a_2, a_1, b, ϕ_0) when $P = 2$) and, hence, it is infeasible to numerically evaluate its mean squared error (MSE). Instead, we run 500 independent Monte-Carlo simulations to measure the empirical MSEs of the proposed PULS estimator. Fig. 3 compares the measured MSEs for estimating the motion-related parameters a_2, a_1 and a_0 with corresponding CRBs. It is seeen that, when SNR $\geq$ 19 dB, the PULS estimator is almost optimal and approaches to the CRB.

B. Performance Evaluation by A Semi-Analytical Dataset

For a more practical evaluation of the proposed speed estimator, we simulated a high-speed read-head scenario by using a semi-analytical simulator (see Fig. 4) by accounting for the spatially periodic reflectors with real system specifications such as the radiation angle, 3-dB beam width, and transmitting beam pattern. The added measurement noise leads to the SNR of 10 dB.

The simulated speed profile is shown in Fig. 5 (a), which includes one acceleration phase, one deceleration phase and two constant-velocity phases. The speed estimates from the proposed method are denoted by blue circles in Fig. 5 (a) and the red solid line denotes the true speed used in the simulation. To implement the proposed PULS method, we set the PPS order of $P = 2$ in(3) for the received signal over a short

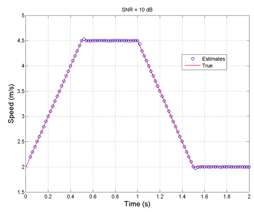

(a) Global speed profile

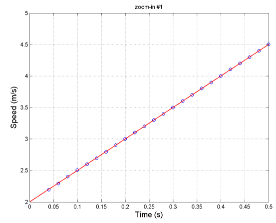

(b) Zoom-in window 1

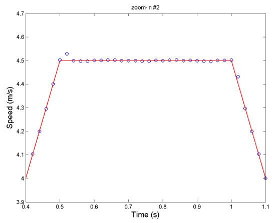

(c) Zoom-in window 2

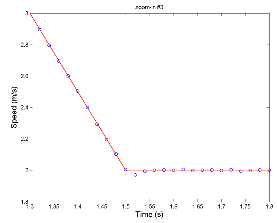

(d) Zoom-in window 3

Fig. 5. Simulated speed profile and speed estimation results by the proposed PULS estimator.

period of 20 ms. Then, the PULS method uses the sampled signal over a given period, estimates the phase parameters and then maps these estimates into the speed estimate.

One can inspect the speed estimation results in three time intervals at $[0,\ 0.5]$s, $[0.4,\ 1.1]$s and $[1.3,\ 1.8]$s, respectively, in Fig. 5 (b) - (d). It is seen that the proposed estimator can track the speed in all three (acceleration, deceleration and constant-velocity) phases. In Fig. 5 (b) and (c), there is an over-shooting issue during the transition from the acceleration phase to the constant-velocity phase. The reason is because, at the transition phase, the sliding window we used to extract the phase information includes sampled signals from the acceleration phase and constant-velocity phase and, hence, there is a model-order change in the signal model of (3), i.e., $P = 2$ of the acceleration phase to $P = 1$ of the constant-velocity phase. This over-shooting issue can be addressed by locating the sampling time where a model-order change occurs, which will be addressed in the future.

V. Conclusion

In this paper, we introduced a new signal model to describe the reflected signal from spatially periodic reflectors in the contactless EM encoder system. According to the signal model, we proposed a phase-based speed estimator which makes use of the coupled signal model for additional information on the speed. The proposed PULS estimator first uses the phase unwrapping technique and then fits the extracted phase by the nonlinear least square method to extract the motion-related parameters. Finally, the proposed estimator is numerically verified by the Monte-Carlo simulations and a semi-analytical dataset with real system specifications.

References

[1] J. F. Gieras, Z. J. Piech, and B. Tomczuk, *Linear Synchronous Motors: Transportation and Automation Systems*, CRC Press, Boca Raton, FL, 2011.

[2] B. M. Wilamowski and J. D. Irwin, *The Industrial Electronics Handbook*, CRC Press, Boca Raton, FL, 2011.

[3] S. Valiviita and S. J. Ovaska, "Delayless acceleration measurement method for elevator control," *IEEE Transactions on Industrial Electronics*, vol. 45, no. 2, pp. 364–366, Apr 1998.

[4] S. Valiviita and S. J. Ovaska, "Delayless recursive differentiator with efficient noise attenuation for motion control applications," in *Industrial Electronics Society, 1998. IECON '98. Proceedings of the 24th Annual Conference of the IEEE*, Aug 1998, vol. 3, pp. 1481–1486 vol.3.

[5] S. Valiviita, S. J. Ovaska, and O. Vainio, "Polynomial predictive filtering in control instrumentation: a review," *IEEE Transactions on Industrial Electronics*, vol. 46, no. 5, pp. 876–888, Oct 1999.

[6] S. Barbarossa, A. Scaglione, and G. B. Giannakis, "Product high-order ambiguity function for multicomponent polynomial-phase signal modeling," *IEEE Trans. on Signal Processing*, vol. 46, no. 3, 1998.

[7] P. O'Shea, "A fast algorithm for estimating the parameters of a quadratic FM signal," *IEEE Trans. on Signal Processing*, vol. 52, no. 2, pp. 385–393, Feb. 2004.

[8] P. Wang, I. Djurovic, and J. Yang, "Generalized high-order phase function for parameter estimation of polynomial phase signal," *IEEE Trans. on Signal Processing*, vol. 56, no. 7, pp. 3023–3028, July 2008.

[9] P. Wang, H. Li, I. Djurović, and B. Himed, "Instantaneous frequency rate estimation for high-order polynomial-phase signals," *IEEE Signal Processing Letters*, vol. 16, no. 9, pp. 782–785, September 2009.

[10] M. R. Bell and R. A. Grubbs, "JEM modeling and measurement for radar target identification," *IEEE Trans. Aerosp. Electron. Syst.*, vol. 29, pp. 73–87, Jan. 1993.

[11] S. Palumbo, S. Barbarossa, A. Farina, and M. R. Toma, "Classification techniques of radar signals backscattered by helicopter blades," in *Proceedings of Int. Symp. Digital Signal Process.*, London, UK, July 1996.

[12] F. Gini and G. B. Giannakis, "Hybrid FM-polynomial phase signal modeling: Parameter estimation and Cramér-Rao bounds," *IEEE Trans. on Signal Processing*, vol. 47, no. 2, pp. 363–377, Feb. 1999.

[13] P. Wang, P. V. Orlik, K. Sadamoto, W. Tsujita, and F. Gini, "Parameter estimation of hybrid sinusoidal FM-polynomial phase signal," *IEEE Signal Processing Letters*, vol. 24, no. 1, pp. 66–70, Jan 2017.

[14] S. M. Kay, *Modern Spectral Estimation: Theory and Application*, Prentice Hall, Englewood Cliffs, NJ, 1988.

[15] P. Wang, P. V. Orlik, K. Sadamoto, W. Tsujita, and Y. Sawa, "Cramér-Rao bounds for a coupled mixture of polynomial phase and sinusoidal FM signals," *IEEE Signal Processing Letters*, vol. 24, no. 6, pp. 66–70, June 2017.